Available online at www.sciencedirect.com
SCIENCE DIRECT®
Catena 54 (2003) 235–254
CATENA
www.elsevier.com/locate/catena

Calibration of the LISEM model for a small Loess Plateau catchment

Rudi Hessel[a,c,*], Victor Jetten[a], Liu Baoyuan[b], Zhang Yan[b], Jannes Stolte[c]

[a] *Department of Physical Geography, Utrecht University, PO Box 80115, 3508 TC Utrecht, The Netherlands*
[b] *Department of Resources and Environment, Beijing Normal University, Beijing 100875, China*
[c] *ALTERRA Green World Research, PO Box 47, 6700 AA Wageningen, The Netherlands*

Abstract

The Limburg Soil Erosion Model (LISEM) soil erosion model was calibrated for a 2-km^2 catchment on the Chinese Loess Plateau. The most important calibration factors were saturated conductivity and Manning's *n*. Calibration on catchment discharge was done by using the discharge peak (timing and discharge) followed by an adjustment for the total discharge to obtain the correct amount of sediment output. The results showed that LISEM can be successfully calibrated for a Loess Plateau catchment, and that small runoff events need to be calibrated separately from large runoff events. A separate calibration might even be needed for each event. The model performance was also evaluated using catchment wide spatially distributed data on rill erosion. Rill erosion intensity was mapped in the field and compared to spatial patterns of erosion predicted by LISEM. The simulated erosion patterns do show some resemblance with mapped erosion patterns in a general sense but they are very different in detail. The cause for this can be found in the extremely steep slopes and abrupt slope changes in the catchment. Some of the process descriptions in LISEM are not intended for such an environment, while the grid based kinematic wave routing cannot cope with the abrupt changes in flow conditions. The effects of this are amplified by inaccuracies in the input data and the DEM. For topographically complex catchments it will be very difficult to obtain data that are good enough for an accurate simulation of erosion patterns. This limits the use of a model such as LISEM as a predictive tool for future events. Simulation of different land use scenarios is less problematic, if a known event is used for all scenario simulations.

Keywords: Soil erosion; LISEM; Calibration; Chinese Loess Plateau; Erosion patterns

* Corresponding author. Tel.: +31-317-474268; fax: +31-317-419000.
E-mail address: rudi.hessel@wur.nl (R. Hessel).

0341-8162/$ - see front matter © 2003 Elsevier Science B.V. All rights reserved.
doi:10.1016/S0341-8162(03)00067-5

1. Introduction

Soil erosion rates on the Chinese Loess Plateau are among the highest worldwide. On-site water and soil losses reduce crop yields and so threaten the livelihoods of rural families, while off-site sedimentation poses problems to waterways and reservoirs. The Chinese government acknowledges the erosion problem and promotes comprehensive erosion control. Erosion modelling might be a useful tool to understand and predict erosion and to ultimately find ways to prevent it.

Although theoretically, fully physically based models would not have to be calibrated, in reality it is different. Models are never fully physically based and many authors have demonstrated the need to calibrate physically based erosion models to obtain an acceptable predictive quality (e.g., Jetten et al., 1999). In the case of hydrological/erosion models calibration has mostly been done using measured data at the outlet of the plot or catchment. Recently, however, several authors have pointed to the necessity of calibrating physically based, distributed models in a spatial way (e.g., Jetten et al., 1996; Takken et al., 1999). Such a calibration is a logical step since the main advantage of distributed models over lumped models should be that they are able to predict spatial patterns. Also, there are circumstances where the location of erosion or deposition in a catchment is more important than the precise amount of water/sediment passing the outlet, for example to design effective anti-erosion measures. Takken et al. (1999) applied the Limburg Soil Erosion Model (LISEM; De Roo et al., 1996a,b; Jetten and De Roo, 2001) model to a small catchment in eastern Belgium. Their catchment was not far from the Limburg catchments that were used to develop the LISEM model. Topography, soils and climate are similar in Limburg and eastern Belgium. Hence, there should be no doubt about the applicability of LISEM in their case. Takken et al. (1999) showed that even when outlet data are reasonably reproduced distribution of erosion and deposition might well be predicted incorrectly. It appeared that although the net soil loss was well predicted, the erosion/deposition rates on the individual fields were considerably different from the measured values.

In the present study, the LISEM erosion model was applied to a small catchment on the Chinese Loess Plateau. Many obvious differences in topography, soils and climate exist between this region and the Dutch province of Limburg. The Danangou catchment (Fig. 1) is a typical small (3.5 km^2) Loess Plateau catchment in Northern China with steep slopes and a loess thickness close to 200 m. The soils are mainly silt loams that classify as Calcaric Regosols/Cambisols in the FAO system (Messing et al., 2003). Median grain size of the loess is about 35 μm. The climate is semi-arid, with occasional heavy thunderstorms in summer. In the town of Ansai, 5 km from the Danangou catchment, total average annual rainfall was 513 mm over the period 1971–1998 (data from Ansai County Meteorological Station). Most of the rain (72%) falls in the period June–September. All heavy storms occur in this period. Only during these large storms runoff occurs in the catchment. On average, three to four storms each year are large enough to cause runoff, but the actual number varies widely from year to year. In the Danangou catchment, discharge only occurs during these heavy storms, when peak discharges of over 10 m^3/s can be reached within 15 min of the onset of channel runoff. Such event characteristics make application of a storm-based erosion model logical. The main land uses in the catchment are:

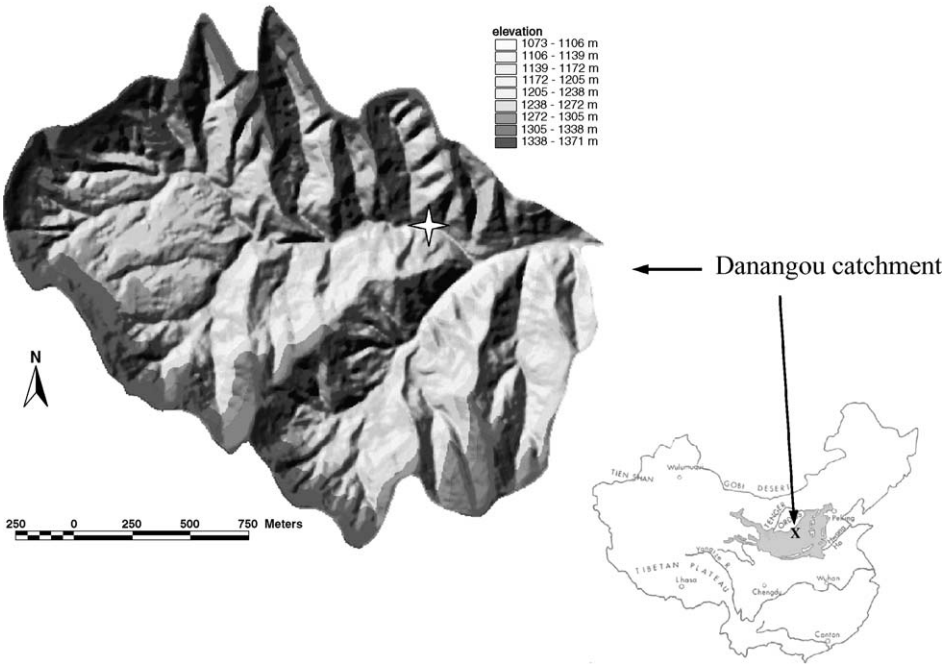

Fig. 1. Elevation map of the Danangou catchment, also showing the approximate position of the Danangou catchment (marked x) on the Loess Plateau (grey area on China map). Shading is used to bring out relief. The position of the weir is indicated with a four-pointed star. The map of China was adapted from Pye (1987).

wasteland (40%), cropland (28%) and fallow (21%). Vegetation cover is generally low, also in croplands, and as the loess soils are susceptible to erosion, very high erosion rates can be reached during the summer storms. Elevation in the catchment ranges from 1070 to 1370 m and the catchment is deeply dissected by gullies, which have slope angles of up to 250%. The croplands are generally located near the water divides above these gullies, and often have slopes in excess of 50%. These steep slopes in the catchment also promote high erosion rates.

The aim of the present study was to evaluate the applicability of the LISEM model for a catchment on the Chinese Loess Plateau. The prediction of both catchment soil loss and spatial erosion patterns was evaluated. To do this, a two-step approach was used. First, the LISEM model was calibrated on runoff and sediment yield measured at the catchment outlet. Then, the simulation results of the calibrated model were evaluated in a spatial way using field observations on erosion patterns.

2. LISEM

LISEM was used in this study because it is a raster-based model and can therefore simulate detailed spatial patterns of erosion. Many soil erosion models do not simulate

erosion patterns at all. The principles of LISEM have been described in several papers (De Roo et al., 1996a,b; Jetten and De Roo, 2001). From these works, it becomes clear that some of the main algorithms of LISEM are only valid for a given range of circumstances. It is therefore possible that the Danangou catchment, because of its gullies that may function both as sinks and source of sediment, and its combination of steep slopes with small-scale land use, provides an environment that LISEM is not able to simulate. Some important characteristics of LISEM that might affect its application in the Danangou catchment will be discussed briefly here.

The first is that in this study a finite difference solution of the Richards equation is used (the SWATRE model; Belmans et al., 1983) to simulate infiltration. The main parameters that determine the infiltration and therefore the amount of runoff and erosion are the saturated conductivity and initial moisture content. De Roo et al. (1996b) showed that LISEM is very sensitive to these parameters. This is also the case with many other erosion models and conductivity and initial moisture content are therefore commonly used for calibration.

The second important characteristic is the way in which transport capacity is calculated. LISEM calculates flow velocity with Manning's equation and subsequently calculates stream power and transport capacity. Since stream power is the product of the velocity and the (energy) slope, the slope angle influences the stream power considerably. According to Govers (1990), the transport capacity equation derived from stream power is valid for slope angles up to 20%, and this will pose one of the largest problems in the application of LISEM to this area. The erosion and deposition are modelled as transport deficits and surpluses and are therefore also strongly determined by the flow conditions.

Another important characteristic of LISEM is that it is a grid-based model. Flow circumstances are determined locally in each grid cell and inertia of water is not taken into account. Thus, while in reality sediment remains in suspension when the slope angle changes abruptly, LISEM may simulate sudden deposition because it assumes that the transport capacity decreases radically. It is therefore possible that the presence of gullies with extreme changes in slope pose problems for the kinematic wave that is used in LISEM to route the water and sediment.

A final feature of LISEM that may be important is that concentrated flow in ditches and ephemeral stream beds can be simulated as a separate process, by defining these features as 'channels.' The channels are assumed impermeable and the channel dimensions and characteristics influence the hydrograph shape considerably.

This study therefore must be seen as a performance test of a physically distributed model under extreme circumstances.

3. Catchment outlet calibration

3.1. Materials and method

For all simulations, LISEM version 1.63 was used with a pixelsize of 10 m and a timestep of 15 s. Since the upper few decimetres of the soil are crucial for infiltration during a storm, 10 calculation layers were used in simulations, with node spacing

Table 1
Multiple regression equations used for predicting initial moisture content (equations provided by Qiu Yang, Research Centre for Eco-Environmental Sciences, Beijing, China)

Depth (cm)	Equation
5	$SW = 0.0712 + 0.0054As + 0.0003S$
15	$SW = 0.0883 + 0.0046As + 0.0001S$
25	$SW = 0.0996 + 0.0051As - 0.00005S$
45	$SW = 0.1172 + 0.0042As - 0.0002S$
75	$SW = 0.1264 + 0.0051As - 0.0004S$

SW = soil water content (volume fraction). As = classified aspect (eight directions), from 0° to 360° in 45° steps respectively 8, 6, 4, 2, 1, 3, 5, 7. S = slope angle (°).

increasing with depth. A single median grain size (D50) of 35 μm is used in all cases in the sediment transport equations of LISEM. As a physically based distributed model, LISEM needs a large amount of input data. During the study period (1998–2000), most of the input parameters needed for the LISEM model were measured repeatedly in the Danangou catchment. Plant and soil characteristics were measured on a fortnightly basis, except for Manning's n, which was measured in two separate campaigns using small runoff plots (Hessel et al., 2003). Soil physical characteristics such as saturated hydraulic conductivity, soil moisture retention curves and the water content–conductivity relationships were determined using samples taken in the catchment. All these measurements are discussed elsewhere in this issue (Wu et al., 2003; Liu et al., 2003; Hessel et al., 2003; Stolte et al., 2003). The field data were converted to input maps for LISEM using the land use map as basis. For variables that clearly also depend on soil type (e.g., cohesion) a combination of land use and soil type was used to extrapolate the measurements. Initial moisture content was predicted with multiple regression equations based on aspect and slope (Table 1). The equations predict moisture content from slope and aspect for different soil depths. The resulting moisture contents are yearly averages and were corrected for particular events using TDR (time domain reflectometry) measurements that were performed close to the date of the event. Rainfall was measured using six tipping bucket rain gauges (1998–2000) and four simple rain gauges that measured total rainfall only (1999–2000). The rain gauges were distributed throughout the catchment. Discharge and sediment concentration were measured at a V-shaped weir built in 1998 (for details, see Van den Elsen et al., 2003). The area upstream of the weir is slightly over 2 km^2, but the total area of the catchment is 3.5 km^2. The position of the weir is indicated in Fig. 1. In the 3-year study period, only four events[1] could be measured. A fifth storm occurred early in the project, but could not be measured because of malfunctioning equipment.

The LISEM model was calibrated first on peak discharge (including time to peak and hydrograph shape) to obtain the correct shape of the hydrograph and after that an adjustment was made to obtain the correct total discharge. Several parameters were used to calibrate on peak discharge, as follows.

[1] The last storm (August 29, 2000) could not be included in this paper as the field data had not yet been analysed.

(1) Saturated conductivity. The saturated conductivity as used in the calibrations was calculated using measured saturated conductivity ($K_{sat(meas)}$) and saturated conductivity determined from the Wind evaporation method (Halbertsma and Veerman, 1997) ($K_{sat(fit)}$), which is extrapolated using the Mualem–van Genuchten equations (see Stolte et al., 2003). This is done with the following equation:

$$K_{sat(est)} = a^{*}K_{sat(fit)} + (1 - a)^{*}K_{sat(meas)} \quad (1)$$

This procedure ensures that $K_{sat(est)}$ is always between $K_{sat(fit)}$ and $K_{sat(meas)}$. The rationale behind this approach is that $K_{sat(fit)}$ might be too low because it does not consider macropore flow, while $K_{sat(meas)}$ is probably too high since during sampling some disturbance is likely and dead-end pores might be cut through.

(2) Initial suction. Initial suction determines the unsaturated conductivity (and thus infiltration) during the start of a rainfall event. Initial suction was only used for calibration if calibrating on saturated conductivity proved insufficient.

(3) Manning's n. Manning's n influences the velocity of runoff and therefore affects the shape and timing of the hydrograph.

(4) Channel length. In LISEM, pixels can be defined that contain a channel characterised by a separate Manning's n. The width of these channels can be defined by the user, but must be smaller than the pixelsize. Flow velocity in the channel will generally be higher as a result of different hydraulic radius. Changing the channel length therefore influences timing and shape of the simulated hydrograph.

All these parameters were changed within reasonable boundaries; that is, within boundaries that could be argued to be realistic given the available amount of data and its uncertainty. K_{sat}, for example, was only allowed to vary between the values measured on the samples and the values determined with the Wind evaporation method. Manning's n was not allowed to be lower than 0.03 or higher than 0.3. Because of the limited number of storms a normal calibration/validation procedure in which a number of events is used for calibration and a number of events for validation was not possible. Instead, each event was calibrated separately. This resulted in three different calibration sets. Each calibration set was validated through its application to the other two events.

Peak discharge calibrations are most suited to evaluate the performance of LISEM because they use time to peak, peak discharge and shape of the hydrograph. Comparing the simulated and observed hydrographs with a goodness-of-fit (e.g., Nash coefficient) was not possible because of a small time shift in the start of the runoff. Therefore, the fitting was done by eye. The total runoff volume calibrations are necessary as sediment loss is calculated as the product of runoff volume and concentration. The total runoff volume calibrations used the peak discharge calibration as a starting point. For the total runoff calibrations, only saturated conductivity was changed.

3.2. Results

The three events that could be measured at the weir occurred on August 1, 1998, August 23, 1998 and July 20, 1999. Table 2 gives a summary of the event characteristics. Table 2 shows that peak discharges were about 5100, 700 and 3700 l/s, respectively. All

Table 2
Event characteristics

	980801	980823	990720
Average rainfall (mm)	15.1	13.0	14.1
Maximum 1-min intensity (mm/h)[a]	69.9	47.2	66.2
Peak discharge (l/s)	5125	701	3720
Total discharge (m^3)	3982[b]	735	3474
Total sediment yield (tonnes)[c]	1280	96	806

[a] The given value is a weighed average of the entire catchment. Intensities at individual rain gauges can be much higher (up to about 120 mm/h for 1-min intervals in the case of both the 980801 and 990720 events).
[b] The hydrograph was incomplete, so this value is estimated by assuming a linear reservoir.
[c] Calculated from total discharge and measured sediment concentration.

events were thus of different magnitude, with the 980801 and 990720 being the least different. Table 2 further suggests that discharge in the Danangou catchment is an intensity phenomenon: average rainfall amounts between the events are not that different, but the lower intensities of the 980823 event clearly result in much lower discharges. This is also shown by the fact that in May 1998, a 2-day rainfall event of 73 mm did not produce runoff at all. Since the hydrograph of the 980801 event is not complete total discharge had to be estimated. The 990720 event was special in that the rainfall amounts in the eastern and western part of the Danangou catchment were very different: at the eastern border, about 30 mm of rain fell, while at the western border (about 2 km away) only 3 mm fell.

Table 3 shows the LISEM input dataset as used for the 990720 event. Datasets for the other events are similar. The availability of input data made it necessary to limit the number of land use based units to 10.

Table 4 shows the calibrated values for the three events of 1998 and 1999. It clearly shows that the calibration gave different results in each case. Most of the differences can, however, be explained from event characteristics.

Table 3
Measured LISEM input dataset (plant and soil characteristics) for the 990720 event

	Crop[a]	Fallow	Orchard	Shrub	Waste	Forest
Aggregate stability (median drop no)	6	5	6	6	8	7.25
Cohesion (kg/cm^2)	0.08	0.10	0.10	0.09	0.11	0.11
Random roughness (cm)	1.75	1.11	1.28	1.03	1.66	0.88
Manning's n	SD[b]	0.079	0.092	0.153[c]	0.091	0.214
Leaf area index	0.06	0.12	1.46	1.25	0.54	1.63
Plant cover (fraction)	0.06	0.10	0.18	0.40	0.23	0.35
Plant height (m)	0.28	0.11	3.1	0.97	0.25	13.6
$K_{sat(meas)}$ (cm/day)	55.9	82.2	96.9	164	153	122
$K_{sat(fitted)}$ (cm/day)	1	1	25	10	5	13
Theta-init	equations from Table 1 used					

[a] Cropland was subdivided in five types. Here, the values for foxtail millet are given. The other types are pearl millet, potato, tall crops (maize, sorghum) and beans.
[b] SD = slope-dependent, Manning's n is calculated from slope angle based on a series of 16 experiments, see Hessel et al. (2003).
[c] Average of wasteland and forest.

Table 4
Peak discharge calibrated values for the 980801, 980823 and 990720 events

	980801	980823	990720
$K_{sat\ a}$[a]	0.90	0.96	0.85
Initial suction (∗original)[b]	1	0.45	1
Manning's n[c]	m − 0.2∗sd	m − 1∗sd	m − 1∗sd
Total channel length (m)	2576	2114	1319
Manning's n channel	0.04	0.06	0.05

[a] See Eq. (1) for explanation.
[b] Original initial suction is the suction that results from the predicted water content, see Table 1. The original value is multiplied by the value in the table. Hence, for the 980823 event the suction becomes smaller, so the soil is wetter.
[c] m: mean of measured data; sd: standard deviation of measured data.

3.2.1. Saturated conductivity

Calibrated saturated conductivity is always much lower than the measured values. A possible explanation for this would be disturbance during sampling. Soil sealing/crusting could also be important. The effect of sealing/crusting is hard to measure on samples taken from the field. It is also possible that in the field complete saturation is not reached. Since for very wet soils the difference in conductivity is very large for a very small change in water content, this could also be an important factor in explaining the much lower conductivities that need to be used during simulation. Another complicating factor is that saturated conductivity appears to increase with an increase in rainfall intensity (e.g., Van Dijck, 2000), which might help explain the differences between the events.

3.2.2. Manning's n

The calibrated values of Manning's n are always lower than measured. The reason for this is not certain, but it seems possible that measured values were too high (Hessel et al., 2003).

3.2.3. Initial moisture content

The 980823 event shows very low saturated conductivities as well as much wetter soils than predicted from the used regression equations. One of the causes of this is likely to be data inaccuracy. The data suggest that a low intensity storm on relatively dry soil did produce discharge. The moisture content of the upper part of the soil profile, in particular, can change rapidly, and the 2-week measurement interval that was used for practical reasons might not be able to reflect these changes accurately. Thus, it is possible that in reality the initial moisture contents were higher than the data indicate, especially since the rainfall data show that about 17 mm of low intensity rain fell 2 days before the event.

3.2.4. Channel length

For the 990720 storm, the 'calibration' channel length was much shorter than for the other events. This can be explained by the fact that this storm only produced high intensity rain in the areas close to the catchment outlet.

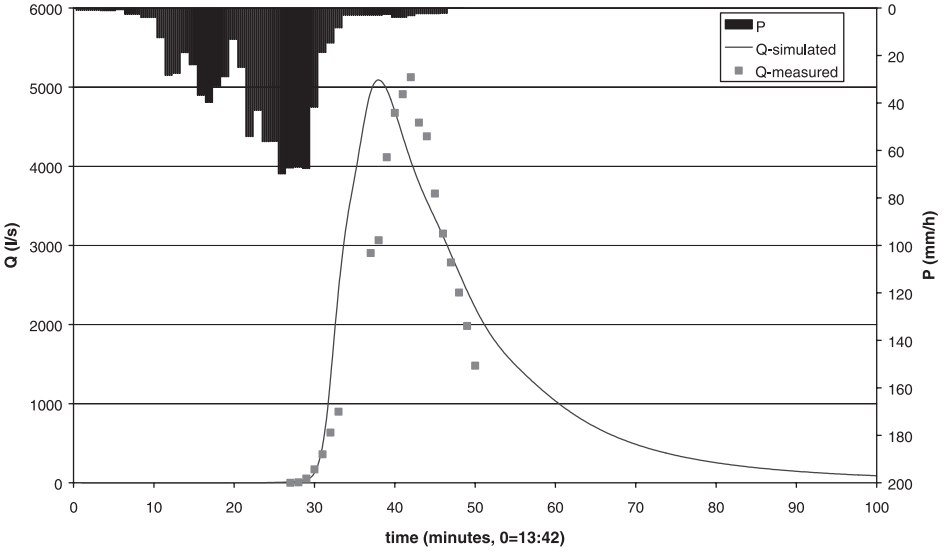

Fig. 2. Precipitation and discharge for the 980801 event.

Figs. 2–4 show the measured discharge as well as the calibrated discharge for each of the events. The graphs show that the simulated discharge peak always occurs too early. Several possible explanations for this can be given.

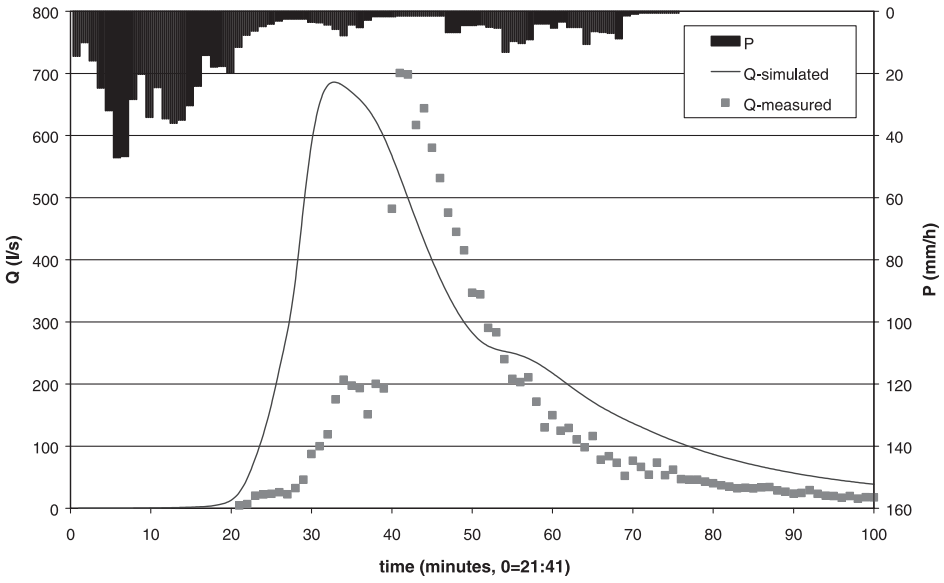

Fig. 3. Precipitation and discharge for the 980823 event.

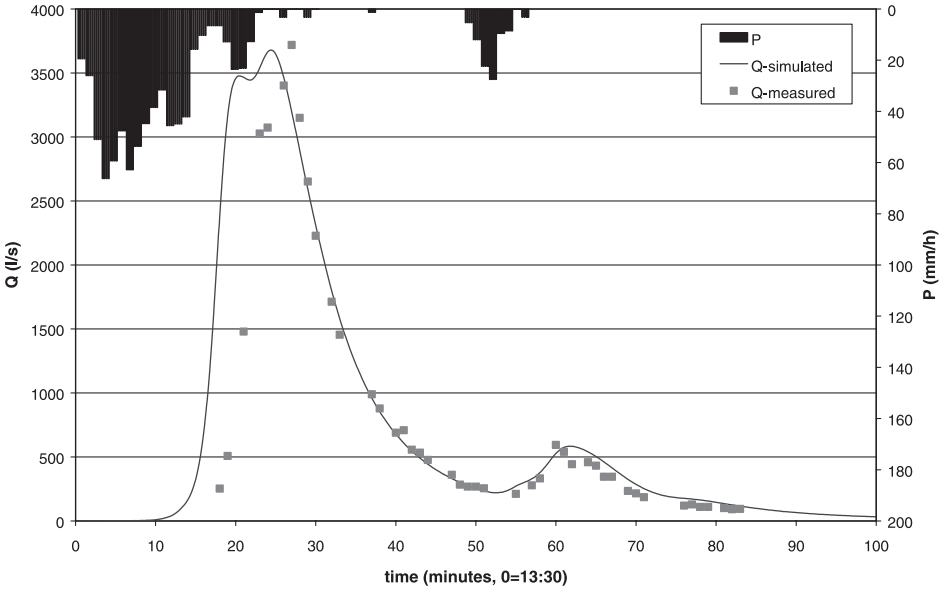

Fig. 4. Precipitation and discharge for the 990720 event.

First, it could be caused by large macropores (such as fissures and sinkholes). The effect of macropores is not simulated with LISEM, since the Richards equation is only valid for matrix flow. In reality, the first runoff on hillslopes might well infiltrate by way of fissures or sinkholes.

Another possible cause would be slope angle. For grid maps, slope angle can be easily calculated when a DEM is available, but the fact that steep slopes increase the actual surface area (or overland distance) is not used. Thus, for steep terrain such as in Danangou, it is conceivable that the actual distance travelled by the water is larger than calculated from the maps. This could cause a too early arrival of the discharge peak as well.

A third possibility would be storage in the channels or infiltration into the channel bed. Since the streams in the catchment are usually dry, depressions in the channel bed have to be filled before the water can advance further. Also, it seems likely that in that case infiltration of channel flow could be important.

Using the calibration data set of one event for the other two events invariably gave worse fits than those presented in Figs. 2–4. The results of this validation are shown in Table 5. Table 5 shows that using the 980801 calibration set for the 990720 event and vice versa still yields acceptable (though worse) results. Still, using the 980823 calibration set for the other two events or vice versa always gives bad results, e.g., using the 980823 calibration dataset for the 980801 event gives a peak discharge of 11809 l/s, while the calibrated value is 5092 l/s (Table 5). The most important parameter that causes these differences is saturated conductivity. This indicates that developing a relationship between rainfall intensity (event magnitude) and saturated conductivity could be worthwhile, since such a relationship could potentially decrease the difference between calibration sets. At present, however, such a relationship is not available. It is therefore concluded that a

Table 5
Results of using the calibrated data sets for the different events

Event	Calibration dataset	Simulated			Measured		
		t_{peak} (min)	Q_{peak} (l/s)	Q_{tot} (m^3)	t_{peak} (min)	Q_{peak} (l/s)	Q_{tot} (m^3)
980801	980801	38	5092	5776	42	5125	3982
980801	980823	38	11,809	12,868			
980801	990720	37.25	4372	4375			
980823	980823	32.75	686	1151	41	701	735
980823	980801	61	29.75	103.7			
980823	990720	74.25	12.48	46.8			
990720	990720	24.5	3678	4285	27	3720	3474
990720	980801	25	4669	5853			
990720	980823	20.25	10,229	12,608			

separate calibration is necessary for events of different magnitudes, and probably even for each event separately.

Fig. 5 shows the calibration results for the total discharge calibration of the 990720 event. The only difference with the peak discharge calibration is that the $K_{sat\ a}$ (see Eq. (1)) has been changed from 0.85 to 0.82. For the 980801, event $K_{sat\ a}$ has been changed from 0.90 to 0.88. For the 980823 event the total discharge calibration has not been performed because the results of the peak calibration were not satisfactory. Comparison of Figs. 4 and 5 shows that calibrating on total runoff leads to a degradation of the fit of the hydrograph. The simulated sediment concentrations show some unexplained wavering, but the average

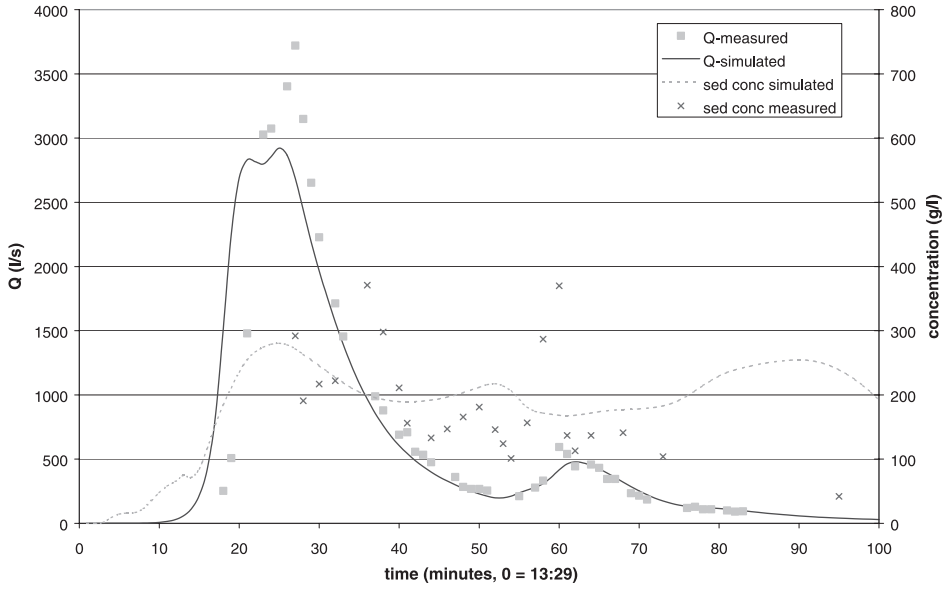

Fig. 5. Results of the total discharge/total erosion calibration of the 990720 event.

Table 6
Summary of the calibration results of the 990720 event

	Measured (Table 1)	Peak discharge calibration	Total discharge calibration
Peak discharge (l/s)	3720	3678	2923
Total discharge (m^3)	3474	4285	3503
Total sediment yield (tonnes)	806	1023	807

sediment concentration is about right. Only at the end of the simulation the predicted sediment concentrations are clearly too high, but at that time the discharge is low so that the total amount of sediment involved is small. Since the average sediment concentration is predicted correctly, the total discharge calibration is at the same time a total erosion calibration.

Table 6 shows that, for the 990720 event, the peak calibration gives good results for peak discharge, but overpredicts total discharge as well as total sediment yield. The total discharge calibration gives both good predictions of total discharge and good total sediment yield, which means that average sediment concentration is also correct, but peak discharge is simulated less well. This shows that one has to perform a slightly different calibration depending on which aim one has with the model.

3.3. Discussion

Our finding that a separate calibration is necessary for small and for large events means that one should be cautious when applying the LISEM model to predict runoff for future events. Such predictions might be possible when these events would be similar in size to the ones used here. Even then initial conditions might well be different, so that one probably has to do simulations with different initial moisture contents. The bigger the event is, the smaller the effect of these initial conditions should be. At present, LISEM might be more suited to evaluate certain land use and management scenarios for their effects on erosion, since in that case all scenarios will use the same rainfall data and the same initial conditions.

4. Erosion pattern evaluation

4.1. Materials and method

At the end of each rainy season (September), the occurrence and intensity of rilling was mapped throughout the 3.5-km^2 catchment. Rill intensity was classified into three classes: slight rill erosion, moderate rill erosion and severe rill erosion. Quantification of the amount of erosion for each class was possible due to a number of measurements of rill frequency, width and depth that was conducted for each rill erosion class. For most years, such mapping will give an aggregated result for all events, but in 1999 only a single rill-producing event occurred so that the rill erosion map made in that year can be used directly to evaluate the performance of LISEM for the 990720 event.

A single erosion plot was installed in 1999 to determine the amount of erosion occurring in arable fields. The plot is assumed representative for the cropland area in the Danangou catchment. Its dimensions were about 34 by 6.5 m, while slope angles ranged from 15% at the top to 55% at the bottom. At the plot, the total amount of water and sediment was measured on an event basis using a division system and barrels. All runoff from the plot was collected in a gutter that drained into the first barrel. If the first barrel was full, 1/11 of the surplus water flowed into the second barrel. Water levels in the barrels were always measured on the day after the rain event, and samples were taken from the barrels to determine sediment concentration. Sediment accumulated in gutter and flume was also taken into account. Since rill measurements were also conducted on the plot it was possible to calculate the total sheet erosion. Often, the fields that are located on the hilltops are convex with a slight concavity in the lower part of the field. For practical reasons, the erosion plot could not end at the lower boundary of the field. It can therefore be assumed that part of the material collected at the plot outlet would redeposit before leaving the field, so that introduction of a sediment delivery ratio for the sheet erosion is necessary.

Using the data from the sediment plot, an estimate of the sheet erosion is obtained. This estimate is expressed as an amount of erosion per unit area of cropland. The rill erosion mapping also gives an amount of erosion per unit area. Therefore, a field erosion-intensity map can be made by combining the two maps. The resulting map can then be compared with the erosion map produced by the LISEM model.

4.2. Results

A minor event that occurred at the sediment plot on July 21, 1999 was used to derive a sheet erosion rate on event basis. The sediment plot is in the western part of the catchment, so that rainfall during the 990720 event was only 3 mm and no runoff occurred on that day. The minor storm did not result in any rill-formation on the sediment plot. Nevertheless, the sediment concentration as determined from the barrels at the bottom of the plot was in excess of 700 g/l, resulting in a sheet erosion rate of 713 tonne/km^2 (7.1 tonne/ha). The sediment delivery ratio of the fields is assumed 0.35. This gives erosion rates (on event basis) of 247 tonne/km^2 for croplands that do not show evidence of rill erosion.

Table 7 shows the average erosion rates obtained from the erosion plot data as well as the rill measurements on the fields. The erosion rate for the ‘no rill erosion’ class is thus a

Table 7
Average observed rill erosion rates (with sheet erosion rates added) and approximate boundaries between classes of rill erosion severity, 1999 data

Erosion class	Erosion rate (tonne/km^2)	Class boundaries (tonne/km^2)
No rill erosion	247	0–800
Slight rill erosion	1446	800–3000
Moderate rill erosion	4818	3000–8000
Severe rill erosion	17,191	above 8000

single event estimate based on sediment plot data, while the other rates are based on rill mapping. The sheet erosion rate was also added to the rill-based measurements of the other classes. Since only one event produced rills in 1999, all these rills must have formed on July 20. The resulting 1999 rill erosion map is shown in Fig. 6A. LISEM produces maps of erosion and deposition rates in tonne/ha. By using the range of measured rill erosion rates for each rill erosion class (Table 7), one can classify the LISEM output map. Since the field mapping only involved erosion and not deposition, it would appear logical to use the LISEM erosion map only. Erosion and deposition can, however, not be treated as separate entities in LISEM simulations; deposition and re-entrainment can occur during the simulation. Thus, the same sediment can be eroded several times and be deposited several times. This provides an explanation for the very large predicted erosion and deposition amounts (e.g., Table 8) and also for the fact that such large amounts have not been observed in the field. Therefore, the net erosion map should be used to assess the performance of the LISEM model in a spatial way. The result should be judged more on patterns than on amounts because during mapping deposition was ignored. The net erosion map was also classified using the values given in Table 7 and is shown in Fig. 6B. Since the rill erosion map (Fig. 6A) only shows erosion on fields, only the cropland areas were used for classification of the LISEM net erosion map.

Comparing the maps in Fig. 6 it is obvious that both maps have the highest erosion rates in the southeastern part of the catchment. This is also in agreement with the observed distribution of rainfall on 990720, since there was a strong spatial trend in rainfall from east (30 mm) to west (3 mm). Closer inspection shows that though the overall pattern is similar, the pattern in detail is very different.

The simulated erosion and deposition for different land uses are given in Table 8. Table 8 shows that according to the simulations the major sediment sources are cropland and fallow land, while the major sink is wasteland. According to the simulation sediment yield from cropland is 2171 tonnes, while according to the rill erosion mapping the total amount of field erosion is 805 tonnes. Field observations do not indicate large erosion amounts on fallow land. Table 8 also shows that 6389 tonnes of sediment is deposited in the valleys, which is almost 70% of all sediment entering them. According to the table, most deposition occurs in valleys with wasteland. Such very high deposition rates have never been observed in the Danangou catchment, thus the erosion rates must also be too high (as the model is calibrated on total sediment yield). Both Fig. 6 and Table 8 therefore suggest that LISEM does not simulate the sediment sources correctly. Summarizing, LISEM over-predicts the erosion on the croplands and compensates this with too much deposition in the valleys. It might be possible to change this by calibrating on cohesion in such a way that total sediment yield remains the same but the distribution of erosion changes. Such calibration has not yet been performed.

4.3. Discussion

Many explanations are possible for the discrepancy between observed and simulated erosion rates and patterns inside the catchment (see, e.g., the discussion by Takken et al., 1999). For the topographically complex Danangou catchment the following factors are likely to be important.

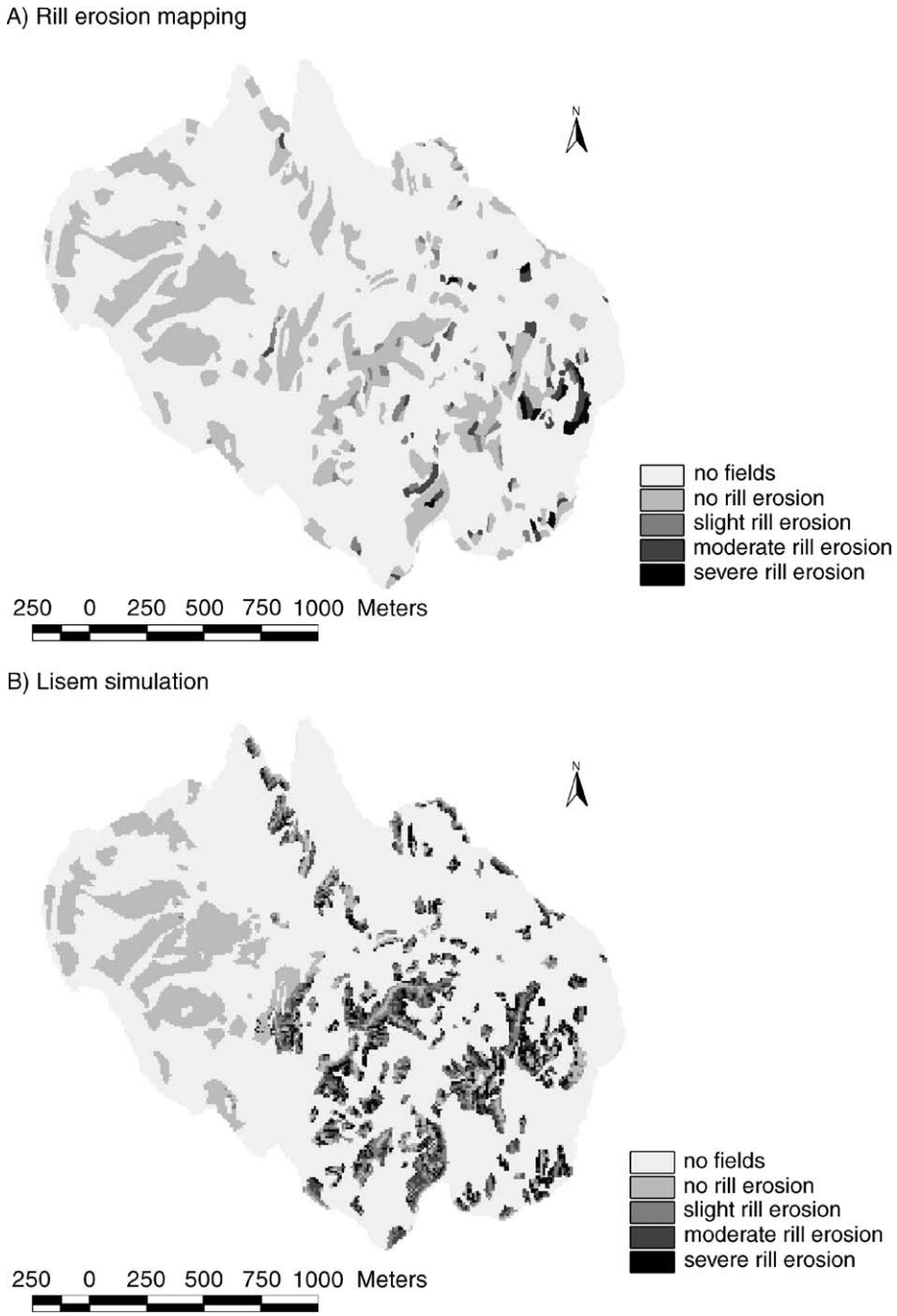

Fig. 6. (A) Mapped rill erosion of 1999. Pixelsize is 5 m. (B) LISEM simulation results for the 990720 event. This map gives a classified map of the net erosion (erosion–deposition). Pixelsize is 10 m. For both maps, the classification scheme given in Table 7 was used.

Table 8
Distribution of erosion (tonnes) according to LISEM simulation

Land use, % of catchment occupied	Erosion	Deposition	Yield	Yield to valleys	Erosion/deposition in valleys
Crop (28%)	4224	− 2053	2171	1957	214
Orchard (1%)	28	− 21	7	4	3
Woodland (9%)	373	− 1335	− 962	− 400	− 562
Wasteland (40%)	9079	− 11,443	− 2365	3463	− 5828
Vegetables (1%)	49	− 11	38	12	26
Fallow (21%)	4932	− 905	4027	4269	− 242
Total	18,685	− 15,768	2917	9305	− 6389

Negative sign indicates deposition. Here, all pixels with an upstream area of more than 1 ha are assumed valleys.

4.3.1. DEM inaccuracy

This is one of the most obvious reasons and also probably one of the most important factors since the flow direction, as used in the model, is derived from the DEM. The flow direction, in turn, determines where erosion will occur according to the model. On relatively flat areas, the tillage direction can determine the direction of water flow (Ludwig et al., 1996; Takken et al., 1999; Van Dijck, 2000), and slope determined from the DEM is than more or less irrelevant (except were furrows overflow). The tillage direction problem is unlikely to be important for steep terrain such as the Danangou catchment. Nevertheless, also in steep terrain, the flow direction is not determined by the average slope of a pixel-sized piece of land. The Danangou DEM (Fig. 1) was derived from a topographical map with contour line interval of 5 m (total relief is 300 m) and the 10-m grid size that was used is therefore very 'reasonable' to accurately depict the variations in relief of a 3.5-km^2 catchment. Nevertheless, such a DEM can only provide average slope directions and cannot contain information about much smaller topographic features (like furrows, pathways, gullies, cut-off drains, local escarpments) that have dimensions in the order of several metres or less and determine the direction of water flow in reality. For topographically complex areas such as the Danangou catchment, it is in reality impossible to obtain a DEM with sufficient accuracy to extract flow directions accurately. For topographically less complex areas, it might be possible by mapping topography and flow direction with the use of surveying techniques.

4.3.2. Limitations of LISEM

The pixel-based approach used in LISEM has some consequences for the calculation process. The most important are related to exceedance of thresholds and to inertia. Both problems are generally more pronounced when there is more water, hence in the channels. Often the net erosion map shows an alternation of pixels with high erosion rates and pixels with high deposition rates. A likely cause of this is that erosion and deposition occur when a certain threshold was exceeded. The problem with this is that at present the threshold will be exceeded time and again for certain pixels. This is because the factors that cause the exceedance do not change during simulation, while in reality they do change. In addition, there is apparently not enough inertia in the model. An example: velocity and stream power are calculated for each pixel separately. This means that in the simulation much more abrupt changes of velocity and stream power can occur than in reality, because in

reality the flow will keep part of its velocity and stream power when it for example enters a reach with lower gradient. In the model, this can result in high sedimentation rates, which in reality will not be the case. The effect of the sedimentation is that the water loses much of its sediment and can therefore cause large erosion rates just downstream. Both factors mainly influence the distribution of erosion and might have little influence on total sediment yield.

These effects are more pronounced for topographically complex areas with strong alternations in slope angle and are at least partly caused by the grid-based approach itself. They can therefore be only partly solved by changing computation procedures.

4.3.3. Incomplete or incorrect process descriptions

No sediment transport equations for slopes of more than 20% were available from the literature. In fact, all currently available erosion models are limited by this, whether they use transport capacity based on bed-load principles or stream power. Such slope angles are, however, very common in the Danangou catchment. More research into transport capacity on steep slopes is needed. In addition, when errors appear to be systematic there might be incomplete process descriptions in LISEM. The fact that the discharge peak always seems to arrive too early might indicate this. Incomplete and incorrect process descriptions might affect both distribution and amount of erosion. As Beven (2001) points out, such errors in theory might be masked by calibration and can therefore be hard to find.

4.3.4. Data inaccuracy

There can be inaccuracies in the data used to evaluate model performance as well as in the input data for the model. Inaccuracies in the data used for evaluation can stem from two sources. The first is the estimation of sheet erosion by using the sediment plot data, for example by choosing a sediment delivery ratio. This might affect the amount of erosion, but not the pattern. The second is mapping inaccuracy and might affect mapped patterns, e.g., because mapping is done by classifying portions of fields and not on a pixel-by-pixel basis. Inaccuracies in input data can be caused by several factors. The first is incorrect measurements. For example, erosion in our simulation seems to be mainly determined by slope angle and less by differences in land use. This might reflect reality, but might also be caused by the fact that cohesion does not seem to change much from one land use to the next (Table 3). Inaccuracies can also be caused by non-representative measurements. Input data for the LISEM model were collected on fields that were supposed to be representative of their respective land uses. Finally, some properties (e.g., soil moisture content) are liable to rapid fluctuations, while others (e.g., saturated conductivity) are notoriously heterogeneous in space. Simulation results also indicated that the rainfall distribution has large influence on simulated runoff and erosion. This is a fundamental problem with distributed modelling; it is impossible to accurately represent existing spatial patterns for all variables. Nowadays, distributed models can contain several tens of thousands of pixels for which the different calculations are performed. Data on saturated conductivity, soil roughness, plant characteristics, etc., are needed for all these pixels. Furthermore, even if such data were available one can for reasons of spatial variability and up-scaling seriously question if the used values are indeed representative for the given pixel. It seems likely that the actual amount of runoff and erosion occurring is controlled by many variations in

parameters operating on sub-grid scale. One has to face reality—it is, in fact, not possible to collect enough input data, nor is it likely to be possible in the future.

Often, a combination of factors could be operating, so that it will be difficult to find out what exactly causes an observed discrepancy between simulation and measurement. Obtaining data that are more accurate (such as a better cohesion map) could in principle solve some of the problems mentioned above. In practice, however, this can be very difficult. To evaluate the LISEM model (or any other physically based, distributed erosion model) in a spatial way, very detailed data both on model input and on erosion and deposition patterns distribution are needed. Such datasets are very hard to obtain for catchment-size areas, especially when topography is complex. It seems therefore unrealistic to aim at a pixel-by-pixel comparison of simulated and measured erosion. Data for the catchment outlet are easier to obtain, so that calibration on the outlet alone will often be the only possibility. Our data, however, confirm the findings of Takken et al. (1999) that an erosion model calibrated on outlet data might well predict spatial patterns incorrectly. Furthermore, even if the necessary data for spatial evaluation were available there is no guarantee that simulated erosion patterns will match observed erosion patterns. This is because errors in model theory or structure as well as problems caused by the grid-based approach itself can also result in incorrectly simulated erosion patterns. Probably, these problems can never be solved completely for complex catchments. For such areas, process-based distributed erosion models can help increase our understanding of erosion, but they might never be able to accurately predict erosion.

5. Conclusions

Calibration of the LISEM soil erosion model for a small catchment on the Chinese Loess Plateau showed that the LISEM model can in principle be applied to the Chinese Loess Plateau. However, the results also show that a separate calibration is needed for low-magnitude and high-magnitude events and probably even for each event. This limits the usefulness of LISEM as a predictor of future discharge. Simulation of different land use scenarios is less problematic, since in scenario analysis an individual known event can be used. Rill erosion intensity was mapped in the field and compared to LISEM simulations of erosion distribution. This comparison shows that the general appearance of simulated and mapped erosion patterns is similar, but also that the patterns are very different in detail. Many causes for this are possible, but it appears that:

(i) Current process descriptions are not well suited to simulate erosion processes on steep slopes.
(ii) The raster based approach of LISEM has the advantage to produce detailed erosion patterns, but the disadvantage is that in combination with the kinematic wave, abrupt changes in flow conditions give unrealistic results.
(iii) At present, the datasets of model input and erosion patterns are not good enough for complex catchments. In particular, inaccuracies in input data and DEM are likely to be important.

The evaluation of catchment soil loss and spatial erosion patterns as simulated by LISEM shows that there are severe limitations in applying such a model for this environment, especially with respect to predicting erosion patterns and future events. Simulation of different land use scenarios might be less problematic if a known event is used for all simulations. Even so, scenario predictions should be done with extreme care and should take into account the factors described above.

Acknowledgements

The research described in this paper was carried out as part of the EU project EROCHINA (contract number: IC18-CT97-0158) and was funded by the EU. We would like to thank Qiu Yang from RCEES for providing us multiple regression equations to predict soil moisture content from aspect and slope and Dr. Theo van Asch for useful comments on earlier versions of the manuscript. The manuscript also benefited from the comments of two anonymous referees.

References

Belmans, C., Wesseling, J.G., Feddes, R.A., 1983. Simulation model of the water balance of a cropped soil: SWATRE. Journal of Hydrology 63, 271–286.

Beven, K., 2001. On modelling as collective intelligence. Hydrological Processes 15, 2205–2207.

De Roo, A.P.J., Wesseling, C.G., Ritsema, C.J., 1996a. LISEM: a single-event physically based hydrological and soil erosion model for drainage basins: I. Theory, input and output. Hydrological Processes 10, 1107–1117.

De Roo, A.P.J., Offermans, R.J.E., Cremers, N.H.D.T., 1996b. LISEM: a single-event physically based hydrological and soil erosion model for drainage basins: II. Sensitivity analysis, validation and application. Hydrological Processes 10, 1119–1126.

Govers, G., 1990. Empirical relationships for transport capacity of overland flow. IAHS Publication 189, 45–63.

Halbertsma, J.M., Veerman, G.J., 1997. Determination of the unsaturated conductivity and water retention characteristic using the Wind's evaporation method. In: Stolte, J. (Ed.), Manual for Soil Physical Measurements. Technical Document, vol. 37. DLO Winand Staring Centre, Wageningen, pp. 47–55.

Hessel, R., Jetten, V., Zhang, G., 2003. Estimating Manning's *n* for steep slopes. Catena 54, 77–91. (doi:10.1016/S0341-8162(03)00058-4)

Jetten, V., De Roo, A.P.J., 2001. Spatial Analysis of erosion conservation measures with LISEM (Ch. 14). In: Harmon, R., Doe, W.W. (Eds.), Landscape Erosion and Evolution Modeling. Kluwer Academic Plenum, New York, pp. 429–445.

Jetten, V., Boiffin, J., De Roo, A., 1996. Defining monitoring strategies for runoff and erosion studies in agricultural catchments: a simulation approach. European Journal of Soil Science 47, 579–592.

Jetten, V., De Roo, A., Favis-Mortlock, D., 1999. Evaluation of field-scale and catchment-scale soil erosion models. Catena 37, 521–541.

Liu, G., Xu, M., Wen, Z., 2003. Study on soil characteristics in a small watershed in the hilly-gullied area on the Loess Plateau in China. Catena 54, 31–44. (doi:10.1016/S0341-8162(03)00055-9)

Ludwig, B., Daroussin, J., King, D., Souchère, V., 1996. Using GIS to predict concentrated flow erosion in cultivated catchments. IAHS Publication 235, 429–436.

Messing, I., Chen, L.D., Hessel, R., 2003. Soil conditions in a small catchment on the Loess Plateau in China. Catena 54, 45–58. (doi:10.1016/S0341-8162(03)00056-0)

Pye, K., 1987. Aeolian Dust and Dust Deposits. Academic Press, London. 334 pp.

Stolte, J., van Venrooi, B., Zhang, G., Trouwborst, K.O., Liu, G., Ritsema, C.J., Hessel, R., 2003. Land-use

induced spatial heterogeneity of soil hydraulic properties on the Loess Plateau in China. Catena 54, 59–75. (doi:10.1016/S0341-8162(03)00057-0)

Takken, I., Beuselinck, L., Nachtergaele, J., Govers, G., Poesen, J., Degraer, G., 1999. Spatial evaluation of a physically-based distributed erosion model (LISEM). Catena 37, 431–447.

Van den Elsen, E., Hessel, R., Liu, B., Trouwborst, K.O., Stolte, J., Ritsema, C.J., Blijenberg, H., 2003. Discharge and sediment measurements at the outlet of a watershed on the Loess Plateau of China. Catena 54, 147–160. (doi:10.1016/S0341-8162(03)00062-6)

Van Dijck, S., 2000. Effects of agricultural land use on surface runoff and erosion in a Mediterranean area. Netherlands Geographical Studies 263, 256.

Wu, Y., Xie, K., Zhang, Qi., Zhang, Y., Xie, Y., Zhang, G., Zhang, W., Ritsema, C.J., 2003. Crop characteristics and their temporal change on the Loess Plateau of China. Catena 54, 7–16. (doi:10.1016/S0341-8162(03)00053-3)